The Influence of the Complexation of Sodium and Lithium Triflate† on the Self-assembly of Tubular-supramolecular Architectures Displaying a Columnar Mesophase Based on Taper-shaped Monoesters of Oligoethylene Oxide with 3,4,5-Tris[*p*-(*n*-dodecan-1-yloxy)benzyloxy]benzoic Acid and of their Polymethacrylates

Virgil Percec,*[a] James A. Heck,[a] Dimitris Tomazos[a] and Goran Ungar[b]
[a] *Department of Macromolecular Science, Case Western Reserve University, Cleveland, OH 44106-2699, USA*
[b] *Department of Engineering Materials and Centre for Molecular Materials, The University of Sheffield, Sheffield, UK S1 3DU*

The monoesters of mono-(**1a**), di-(**1b**), tri-(**1c**) and tetra-(**1d**) ethylene glycol with 3,4,5-tris[*p*-(*n*-dodecan-1-yloxy)benzyloxy]benzoic acid (**1**), the polymethacrylates derived from them (**2**) and the complexes of both **1** and **2** with $LiCF_3SO_3$ and $NaCF_3SO_3$ self-assemble into cylindrical supramolecular architectures which exhibit a hexagonal columnar (Φ_h) mesophase. The generation of the Φ_h mesophase depends on the stabilization of this assembly by *endo*-recognition in the core of the cylinder (H-bonding and ionic interactions) and *exo*-recognition that occurs between the tapered groups and also between the cylinders (*i.e.*, the hexagonal arrangement of the columns). The low molecular weight compounds **1** are able to complex more salt in the Φ_h mesophase and have larger increases in Φ_h–isotropic transition temperature ($T_{\Phi h-i}$) per increase in salt concentration than the corresponding polymethylcrylates **2** derived from them. Molecular modelling appears to indicate that positional and conformational restrictions imposed by both the tapered side groups and the polymer backbone are responsible for these results. Both the polymers and the low molar mass compounds have their $T_{\Phi h-i}$ shifted to lower temperatures and allow more $LiCF_3SO_3$ to be complexed with the increase in the number of oxyethylene segments present in the flexible spacer. A comparison of the difference in the effectiveness of the Li cation *versus* the Na cation in providing increased stabilization of the Φ_h mesophase does not show any significant differences between the two cations.

Molecular-recognition-directed self-assembly of supramolecular architectures[1] and self-synthesis[2] are two of the most active areas of research in contemporary chemistry. Recently we became interested in the self-assembly of cylindrically shaped supramolecular architectures by using a combination of *exo*- and *endo*-recognition,[3,4] or *exo*-recognition and a polymerization process.[5] The principles of this research have been discussed in detail elsewhere.[3,4,5b]

The monoesters of mono-(**1a**), di-(**1b**), tri-(**1c**) and tetra-(**1d**) ethylene glycol with 3,4,5-tris[*p*-(*n*-dodecan-1-yloxy)benzyloxy]benzoic acid (**1**), the polymethacrylates derived from them (**2**) (Fig. 1) and the complexes of both **1** and **2** with $LiCF_3SO_3$ self-assembly into cylindrical supramolecular architectures which exhibit a hexagonal columnar (Φ_h) mesophase. **1**, **2** and the complexes of $LiCF_3SO_4$ have been previously characterized by a combination of differential scanning calorimetry (DSC), X-ray scattering experiments, density measurements, and thermal optical polarized microscopy.[4] With the additional information provided by molecular modelling, a representative model of a self-assembled supramolecular cylinder with hydrophilic oligooxyethylene segments comprising the core of the cylinder and the hydrophobic aromatic and paraffinic groups being concentrated at the periphery region of the cylinder was proposed. A representation of this cylindrical assembly and of its complex with $LiCF_3SO_3$ is shown in Fig. 2. This self-assembly process is proposed to occur *via* a combination of microsegregation of the hydrophobic and hydrophilic segments of the molecules and regular packing of the tapered groups into a cylindrical shape which resembles an inverse micelle. The generation of the Φ_h mesophase is

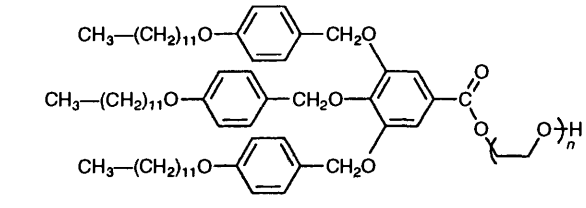

n = 1 : **1a**
n = 2 : **1b**
n = 3 : **1c**
n = 4 : **1d**

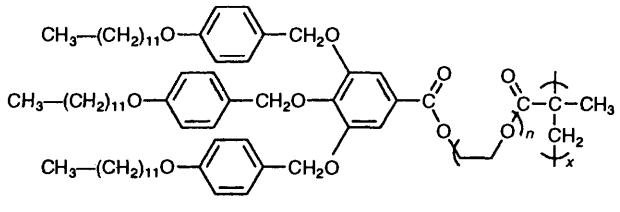

n = 1 : **2a**
n = 2 : **2b**
n = 3 : **2c**
n = 4 : **2d**

Fig. 1 Structures of ω-hydroxyoligooxyethylene 3,4,5-tris[*p*-(*n*-dodecan-1-yloxy)benzyloxy]benzoates (**1a–d**), and of the polymethacrylates based on them (**2**)

† Trifluoromethanesulfonate.

Table 1 Thermal transitions of the complexes of **1** and **2** with various amounts of $LiCF_3SO_3$ and $NaCF_3SO_3$ (Φ_h = hexagonal columnar mesophase; k_1, k_2, k_3 = crystalline phases; i = isotropic phase; c = crystallization occurs during heating; g = glassy phase). The data are from the first heating, second heating and first cooling DSC scans

Compd.	Salt added to **1** or **2**		Thermal transition (°C) and corresponding enthalpy changes (in parentheses, kcal mol^{-1})[a]		
	Type	Moles	1st heating scan	2nd heating scan	1st cooling scan
1a	$LiCF_3SO_3$	0.00	c 46 (−1.8) k_2 58 (4.9) k_1 71 (0.39) Φ_h 85 (0.73) i	$k_3$4.5 (1.8) c 48 (−1.1) k_2 56 (2.1) k_1 72 (1.2) Φ_h 84 (0.70) i	i 76 (0.76) Φ_h 25 (4.2) k_1
1a	$LiCF_3SO_3$	0.03	k_1 53, 72 (13.2)[b] Φ_h 86 (0.86) i	c 46 (−1.3) k_1 57 (4.9) Φ_h 86 (0.71) i	i 78 (0.73) Φ_h 23 (3.9) k_1
1a	$LiCF_3SO_3$	0.06	k_1 50, 71 (13.4)[b] Φ_h 87 (0.70) i	k_1 52 (5.4) Φ_h 87 (0.74) i	i 79 (0.69) Φ_h 17 (3.6) k_1
1a	$LiCF_3SO_3$	0.09	k_1 50, 70 (13.9)[b] Φ_h 87 (0.58) i	k_1 51 (5.9) Φ_h 88 (0.58) i	i 80 (0.69) Φ_h15 (3.6) k_1
1a	$LiCF_3SO_3$	0.12	k_1 54, 72 (13.2)[b] Φ_h 89 (0.57) i	k_1 52 (5.2) Φ_h 90 (0.58) i	i 79 (0.55) Φ_h 12 (3.1) k_1
1a	$LiCF_3SO_3$	0.15	k_1 50, 70 (13.4)[b] Φ_h 89 (0.53) i	k_1 52 (6.3) Φ_h 91 (0.57) i	i 81 (0.59) Φ_h 11 (3.7) k_1
1a	$LiCF_3SO_3$	0.18	k_1 51, 69 (13.3)[b] Φ_h 88 (0.51) i	k_1 53 (5.5) Φ_h 92 (0.53) i	i 81 (0.53) Φ_h 13 (3.4) k_1
1a	$LiCF_3SO_3$	0.21	k_1 50, 64 (13.2)[b] Φ_h 96 (0.36) i	k_1 55 (6.3) Φ_h 96 (0.44) i	i 84 (0.38) Φ_h 21 (5.6) k_1
1a	$LiCF_3SO_3$	0.24	k_1 49, 65 (12.8)[b] Φ_h 97 (0.38) i	k_1 54 (5.5) Φ_h 94 (0.44) i	i 86 (0.43) Φ_h 19 (4.3) k_1
1a	$LiCF_3SO_3$	0.27	k_1 50, 63 (12.7)[b] Φ_h 98 (0.49) i	k_1 54, 64 (5.4)[b] Φ_h 97 (0.40) i	i 88 (0.45) Φ_h 21 (4.1) k_1
1a	$LiCF_3SO_3$	0.30	k_1 49, 63 (13.3)[b] Φ_h 99 (0.41) i	k_1 53, 66 (5.23)[b] Φ_h 98 (0.51) i	i 89 (0.41) Φ_h 21 (4.0) k_1
1b	$LiCF_3SO_3$	0.00	k_1 66 (8.3) Φ_h 73 (0.49) i	k_1 66 (8.3) Φ_h 73 (0.45) i	i 65 (0.74) Φ_h 35 (9.5) k_1
1b	$LiCF_3SO_3$	0.08	k_1 66 (11.7) Φ_h 79 (0.65) i	k_1 64 (9.6) Φ_h 79 (0.65) i	i 71 (0.57) Φ_h 33 (9.8) k_1
1b	$LiCF_3SO_3$	0.16	k_1 66 (11.5) Φ_h 82 (0.57) i	k_1 61 (9.5) Φ_h 83 (0.54) i	i 74 (0.50) Φ_h 33 (9.6) k_1
1b	$LiCF_3SO_3$	0.24	k_1 64 (11.8) Φ_h 84 (0.47) i	k_1 57 (10.2) Φ_h 85 (0.61) i	i 76 (0.49) Φ_h 33 (9.5) k_1
1b	$LiCF_3SO_3$	0.32	k_1 62 (11.0) Φ_h 85 (0.45) i	k_1 55 (9.1) Φ_h 86 (0.55) i	i 79 (0.49) Φ_h 33 (9.2) k_1
1b	$LiCF_3SO_3$	0.40	k_1 62 (11.1) Φ_h 86 (0.49) i	k_1 55 (9.8) Φ_h 89 (0.40) i	i 78 (0.30) Φ_h 33 (9.2) k_1
1c	$LiCF_3SO_3$	0.00	k_1 56 (18.9) Φ_h 63 (0.80) i	k_1 56 (13.3) Φ_h 61 (0.75) i	i 54 (0.72) Φ_h 34 (14.7) k_1
1c	$LiCF_3SO_3$	0.10	k_1 58 (13.6) Φ_h 73 (0.72) i	k_1 53 (13.3) Φ_h 64 (0.68) i	i 55 (0.46) Φ_h 27 (12.2) k_1
1c	$LiCF_3SO_3$	0.20	k_1 56 (13.4) Φ_h 84 (0.51) i	k_1 56 (14.1) Φ_h 83 (0.57) i	i 76 (0.54) Φ_h 32 (13.7) k_1
1c	$LiCF_3SO_3$	0.30	k_1 54 (13.6) Φ_h 90 (0.52) i	k_1 54 (13.8) Φ_h 89 (0.50) i	i 82 (0.47) Φ_h 30 (13.1) k_1
1c	$LiCF_3SO_3$	0.40	k_1 43, 54 (16.9)[b] Φ_h 99 (0.48) i	k_1 54 (13.4) Φ_h 97 (0.40) i	i 89 (0.43) Φ_h 28 (13.3) k_1
1c	$LiCF_3SO_3$	0.50	k_1 52 (13.8) Φ_h 105 (0.47) i	k_1 52 (12.9) Φ_h 103 (0.38) i	i 97 (0.29) Φ_h 30 (12.5) k_1
1c	$LiCF_3SO_3$	0.60	k_1 51 (12.9) Φ_h 111 (0.26) i	k_1 52 (12.4) Φ_h 108 (0.33) i	i 102 (0.25) Φ_h 30 (11.9) k_1
1c	$LiCF_3SO_3$	0.70	k_1 52 (12.5) Φ_h 115 (0.11) i	k_1 52 (12.1) Φ_h 113 (0.27) i	i 106 (0.22) Φ_h 29 (11.3) k_1
1c	$LiCF_3SO_3$	0.80	k_1 53 (12.2) Φ_h 123 (0.24) i	k_1 53 (11.1) Φ_h 117 (0.27) i	i 109 (0.30) Φ_h 28 (10.4) k_1
1c	$LiCF_3SO_3$	0.90	k_1 52 (11.9) Φ_h 128 (0.22) i	k_2 16 (0.18) k_1 50 (9.1) Φ_h 115 (0.24) i	i 110 (0.26) Φ_h 25 (7.8) k_1
1c	$LiCF_3SO_3$	1.00	k_1 52 (12.2) Φ_h 134 (0.24) i	k_2 14 (0.34) c 26 (−0.64) k_1 47 (6.4) Φ_h 106 (0.14) i	i 97 (0.12) Φ_h 21 (5.1) k_1
1c	$LiCF_3SO_3$	1.20	k_1 51 (11.6) Φ_h 138 (0.09) i	k_2 13 (1.5) c 27 (−1.4) k_1 46 (2.7) Φ_h 74 (0.10) i	i 62 (0.06) Φ_h 13.0 (1.3)[d] k_1
1c	$NaCF_3SO_3$	0.10	k_1 52 (15.1) Φ_h 75 (0.72) i	k_1 53 (14.4) Φ_h 75 (0.69) i	i 69 (0.70) Φ_h 32 (14.0) k_1
1c	$NaCF_3SO_3$	0.20	k_1 51(13.8) Φ_h 85 (0.65) i	k_1 51 (13.6) Φ_h 85 (0.54) i	i 79 (0.54) Φ_h 29 (13.4) k_1
1c	$NaCF_3SO_3$	0.30	k_1 51 (13.9) Φ_h 93 (0.43) i	k_1 51 (13.4) Φ_h 92 (0.49) i	i 86 0.53) Φ_h 28 (12.6) k_1
1c	$NaCF_3SO_3$	0.40	k_1 51 (13.6) Φ_h 98 (0.67) i	k_1 49 (12.4) Φ_h 98 (0.44) i	i 91 (0.44) Φ_h 25 (11.2) k_1
1c	$NaCF_3SO_3$	0.50	k_1 50 (13.6) Φ_h 103 (0.38) i	k_1 49 (12.2) Φ_h 103 (0.35) i	i 97 (0.39) Φ_h 25 (11.2) k_1
1c	$NaCF_3SO_3$	0.60	k_2 30 (3.9) k_1 50 (12.6) Φ_h 112 (0.25) i	k_1 50 (12.4) Φ_h 111 (0.33) i	i 104 (0.32) Φ_h 25 (11.1) k_1
1c	$NaCF_3SO_3$	0.70	k_1 51 (11.8) Φ_h 113 (0.18) i	k_1 49 (11.4) Φ_h 115 (0.27) i	i 110 (0.26) Φ_h 25 (11.1) k_1
1c	$NaCF_3SO_3$	0.80	k_1 49 (11.4) Φ_h 116[c] i	k_1 50 (13.7) Φ_h 118 (0.34) i	i 111 (0.28) Φ_h 24 (8.6) k_1
1c	$NaCF_3SO_3$	0.90	k_1 49 (11.2) Φ_h 122 (0.20) i	k_1 51 (10.8) Φ_h131 (0.08) i	i 123 (0.09) Φ_h 25 (7.1) k_1
1c	$NaCF_3SO_3$	1.00	k_1 49 (10.9) Φ_h 126 (0.09) i	k_2 27 (0.88) k_1 50 (10.0) Φ_h 123 (0.14) i	i 116 (0.20) Φ_h 25 (7.1) k_1
1c	$NaCF_3SO_3$	1.10	k_1 50 (10.5) Φ_h 122 (0.07) i	k_2 25 (2.6) k_1 (13.2) Φ_h 115 (0.17) i	i 109 (0.19) Φ_h 14 (7.1) k_1

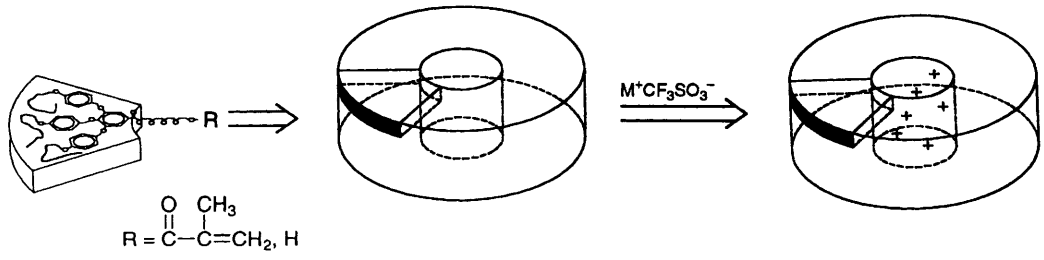

Fig. 2 A tilted side view of the schematic representation of the mono-substituted alcohols **1** and the methacrylate monomers based on them being polymerized covalently or *via* H-bonding to a self-assembled cylindrically shaped supramolecule in the Φ_h phase and the complexation of triflate salts by the oxyethylene segments in the inner core of the assembly

dependent on the stabilization of this assembly by *endo*-recognition in the core of the cylinder (H-bonding and ionic interactions) and *exo*-recognition that occurs between the tapered groups and also between the cylinders (*i.e.*, the hexagonal arrangement of the columns).

In this paper we discuss the changes in the phase behaviour occurring upon complexation of **1** and **2** with $LiCF_3SO_3$ and $NaCF_3SO_3$. The ability to regulate the phase behaviour of side-chain liquid crystals containing various *endo*-receptors *via* molecular recognition of metal salts has previously been

Table 1 (*continued*)

Compd.	Salt added to **1** or **2**		Thermal transition (°C) and corresponding enthalpy changes (in parentheses, kcal mol^{-1})[a]		
	Type	Moles	1st heating scan	2nd heating scan	1st cooling scan
1c	$NaCF_3SO_3$	1.20	k_1 50 (13.6) Φ_h 123 (0.06) i	k_2 31 (0.98) k_1 49 (9.1) Φ_h 121 (0.20) i	i 116 (0.26) Φ_h 23 (7.2) k_1
1d	$LiCF_3SO_3$	0.00	k_1 50 (16.4) Φ_h 59 (0.74) i	k_1 49 (15.5) Φ_h 57 (0.88) i	i 52 (0.78) Φ_h 31 (15.1) k_1
1d	$LiCF_3SO_3$	0.10	k_1 49 (15.0) Φ_h 69 (0.76) i	k_1 48 (15.5) Φ_h 69 (0.68) i	i 64 (0.69) Φ_h 30 (15.0) k_1
1d	$LiCF_3SO_3$	0.20	k_1 48 (14.9) Φ_h 76 (0.74) i	k_1 47 (15.0) Φ_h 74 (0.46) i	i 69 (0.64) Φ_h 29 (14.6) k_1
1d	$LiCF_3SO_3$	0.30	k_1 48 (15.4) Φ_h 82 (0.58) i	k_1 47 (14.6) Φ_h 81 (0.52) i	i 76 (0.52) Φ_h 28 (14.2) k_1
1d	$LiCF_3SO_3$	0.40	k_1 46 (15.0) Φ_h 89 (0.41) i	k_1 49 (14.1) Φ_h 88 (0.46) i	i 83 (0.40) Φ_h 26 (13.5) k_1
1d	$LiCF_3SO_3$	0.50	k_1 45 (15.0) Φ_h 94 (0.27) i	k_1 49 (13.8) Φ_h 94 (0.38) i	i 88 (0.38 Φ_h 25 (13.3) k_1
1d	$LiCF_3SO_3$	0.60	k_1 47 (14.6) Φ_h 100 (0.39) i	k_1 47 (13.6) Φ_h 100 (0.28) i	i 95 (0.36) Φ_h 25 (11.4) k_1
1d	$LiCF_3SO_3$	0.70	k_1 47 (14.3) Φ_h 103 (0.31) i	k_1 47 (13.2) Φ_h 103 (0.24) i	i 97 (0.31) Φ_h 26 (11.9) k_1
1d	$LiCF_3SO_3$	0.80	k_1 46 (14.6) Φ_h 108 (0.36) i	k_1 47 (13.0) Φ_h 107 (0.29) i	i 101 (0.31)Φ_h 25 (12.6) k_1
1d	$LiCF_3SO_3$	0.90	k_1 51 (15.1) Φ_h 111 (0.13) i	k_1 47 (12.7) Φ_h 109 (0.21) i	i 104 (0.22) Φ_h 25 (12.2) k_1
1d	$LiCF_3SO_3$	1.00	k_1 47 (14.2) Φ_h 116 (0.26) i	k_1 47 (12.3) Φ_h 113 (0.19) i	i 108 (0.22) Φ_h 25(12.0) k_1
1d	$LiCF_3SO_3$	1.10	k_1 47 (13.8) Φ_h 118 (0.15) i	k_1 47 (12.1) Φ_h 114 (0.19) i	i 108 (0.22) Φ_h 25 (11.3) k_1
1d	$LiCF_3SO_3$	1.20	k_1 46 (11.0) Φ_h 123 (0.07) i	k_1 47 (9.4) Φ_h 115 (0.05) i	i 108 (0.07) Φ_h 24 (8.8) k_1
1d	$NaCF_3SO_3$	0.10	k_1 50 (15.6) Φ_h 66 (0.91) i	k_1 50 (15.6) Φ_h 65 (0.74) i	i 59 (0.74) Φ_h 31 (15.3) k_1
1d	$NaCF_3SO_3$	0.20	k_1 49 (15.1) Φ_h 72 (0.61) i	k_1 49 (14.8) Φ_h 72 (0.52) i	i 66 (0.65) Φ_h 29 (14.3) k_1
1d	$NaCF_3SO_3$	0.30	k_1 49 (15.1) Φ_h 78 (0.51) i	k_1 49 (14.3) Φ_h 78 (0.49) i	i 72 (0.53) Φ_h 29 (13.7) k_1
1d	$NaCF_3SO_3$	0.40	k_1 48, 56 (14.7)[b] Φ_h 88 (0.45) i	k_1 47, 51 (13.0)[b] Φ_h 87 (0.44) i	i 82 (0.38) Φ_h 26 (12.9) k_1
1d	$NaCF_3SO_3$	0.50	k_1 48 (45.2) Φ_h 89 (0.37) i	k_1 46, 51 (13.0)[b] Φ_h 88 (0.32) i	i 83 (0.34) Φ_h 26 (12.6) k_1
1d	$NaCF_3SO_3$	0.60	k_1 49 (13.6) Φ_h 98 (0.29) i	k_1 47, 52 (12.8)[b] Φ_h 98 (0.24) i	i 91 (0.25) Φ_h 24 (11.8) k_1
1d	$NaCF_3SO_3$	0.70	k_1 46 (20.1) Φ_h 103 (0.24) i	k_1 46 (12.2) Φ_h 103 (0.26) i	i 98 (0.20) Φ_h25 (11.3) k_1
1d	$NaCF_3SO_3$	0.80	k_1 47, 53 (13.1)[b] Φ_h 103 (0.26) i	k_1 48 (11.4) Φ_h 103 (0.25) i	i 97 (0.23) Φ_h 22 (10.1) k_1
1d	$NaCF_3SO_3$	0.90	k_1 47 (12.9) Φ_h 107 (0.22) i	k_1 47 (11.1) Φ_h 107 (0.11) i	i 102 (0.10) Φ_h 23 (9.9) k_1
1d	$NaCF_3SO_3$	1.00	k_1 46, 53 (12.6)[b] Φ_h 113 (0.16) i	k_2 12 (0.25) c 25 (−1.1) k_1 46 (9.3) Φ_h 112 (0.17) i	i 108 (0.20) Φ_h 17 (5.8) k_1
1d	$NaCF_3SO_3$	1.10	k_1 52 (12.0) Φ_h 116 (0.10) i	k_2 12 (0.27) c 26 (−0.82) k_1 46 (8.2) Φ_h 115 (0.07) i	i 113 (0.17) Φ_h 17 (5.0) k_1
1d	$NaCF_3SO_3$	1.20	k_1 52 (11.5) Φ_h 110 (0.06) i	k_2 12 (0.55) c 24 (−1.1) k_1 45 (7.2) Φ_h 110 (0.08) i	i 107 (0.05) Φ_h 15 (4.2) k_1
2a	$LiCF_3SO_3$	0.00	Φ_h 127 (0.30) i	Φ_h 127 (0.30) i	i 110 (0.38) Φ_h
2a	$LiCF_3SO_3$	0.10[d]	Φ_h 110 (0.13) i	—	—
2a	$LiCF_3SO_3$	0.20[d]	Φ_h 104 (0.05) i	—	—
2b	$LiCF_3SO_3$	0.00	g 36 Φ_h 116 (0.38) i	g 37 Φ_h 116 (0.30) i	i 103 (0.38) Φ_h 29 g
2b	$LiCF_3SO_3$	0.10[d]	Φ_h 105 (0.24) i	—	—
2b	$LiCF_3SO_3$	0.20[d]	Φ_h 104 (0.08) i	—	—
2b	$LiCF_3SO_3$	0.30[d]	Φ_h 101 (0.04) i	—	—
2c	$LiCF_3SO_3$	0.00	k_1 48 (3.32) Φ_h 113 (0.43) i	Φ_h 112 (0.43) i	i 103 (0.45) Φ_h
2c	$LiCF_3SO_3$	0.10	Φ_h 116 (0.57) i	Φ_h 115 (0.50) i	i 105 (0.47) Φ_h
2c	$LiCF_3SO_3$	0.20	Φ_h 123 (0.39) i	Φ_h 122 (0.32) i	i 111 (0.35) Φ_h
2c	$LiCF_3SO_3$	0.30	k_1 52 (0.27) Φ_h 117 (0.21) i	Φ_h 124 (0.22) i	i 116 (0.28) Φ_h
2c	$LiCF_3SO_3$	0.40	k_1 48 (0.29) Φ_h 122 (0.19) i	Φ_h 129 (0.14) i	i 118 (0.22) Φ_h
2c	$LiCF_3SO_3$	0.50	k_1 55 (0.50) Φ_h 118 (0.17) i	Φ_h 126 (0.05) i	i 113 (0.09) Φ_h
2d	$LiCF_3SO_3$	0.00	k_1 47 (3.75) Φ_h 103 (0.50) i	Φ_h 99 (0.43) i	i 87 (0.69) Φ_h
2d	$LiCF_3SO_3$	0.10	k_1 43 (3.00) Φ_h 106 (0.45) i	Φ_h 101 (0.47) i	i 88 (0.43) Φ_h
2d	$LiCF_3SO_3$	0.20	Φ_h 111 (0.45) i	Φ_h 106 (0.35) i	i 92 (0.30) Φ_h
2d	$LiCF_3SO_3$	0.30	Φ_h 117 (0.22) i	Φ_h 110 (0.24) i	i 97 (0.25) Φ_h
2d	$LiCF_3SO_3$	0.40	Φ_h 121 (0.15) i	Φ_h 114 (0.19) i	i 98 (0.21) Φ_h
2d	$LiCF_3SO_3$	0.50	Φ_h 112 (0.07) i	Φ_h 112 (0.12) i	i 93 (0.16) Φ_h
2d	$LiCF_3SO_3$	0.60	Φ_h 111 (0.07) i	Φ_h 112 (0.08) i	i 93 (0.13) Φ_h

[a] The molecular weight is weight averaged with the amount of $NaCF_3SO_3$ or $LiCF_3SO_3$ present. [b] Combined enthalpies for overlapped transitions are presented. [c] The transition was undetectable by DSC and the temperature was assigned by thermal optical polarized microscopy at 20 °C/min. [d] Second heating and first cooling transitions could not be determined owing to sample decomposition.

reported from our laboratory.[6] The changes in the phase behaviour of the complexes of **1** and **2** with $LiCF_3SO_3$ and $NaCF_3SO_3$ as a function of the number of oxyethylene units in the spacer and the difference that results when this assembly is formed by a 'molecular' polymer backbone (covalent) or a 'supramolecular' polymer backbone (H-bonding) are discussed. Also, two sets of examples comparing the difference in the effectiveness of the Li and Na cations in providing the stabilization of the supramolecular assembly are presented.

Experimental

The details of the synthesis and characterization of compounds **1a–d** and **2a–d** (shown in Fig. 1) as well as the preparation of their complexes with $LiCF_3SO_3$ and $NaCF_3SO_3$ were reported previously.[4] Molecular modelling was done using CSC Chem3D Plus™ from Cambridge Scientific Computing, Inc.

Results and Discussion

Fig. 1 shows the structures of compounds **1** and **2**. The phase behaviour of the $LiCF_3SO_3$ and $NaCF_3SO_3$ complexes of compounds **1** and **2** was investigated by differential scanning calorimetry (DSC). Representative DSC traces of these complexes have been previously reported and will not be presented here.[4] The results of the DSC analysis of the pure compounds and of their complexes are summarized in Table 1. Representative textures of the Φ_h mesophase of the compounds

1 and **2** as observed under crossed polarizers are shown in Fig. 3. Fig. 3(*a*)–(*c*) show the focal conic and fan-shaped focal conic textures of **1a**, **1d** and **2c**, respectively, in the absence of any complexed salt. Fig. 3(*d*) shows a texture of **2c** with 0.4 mol of added $LiCF_3SO_3$. In all cases the polymers **2** form textures more slowly upon cooling from the isotropic melt into the Φ_h mesophase with smaller domains than the textures formed by their low molecular weight analogues **1**.

The dependence of the phase behaviour of complexes of **1** and **2** on the amount of salt is shown in Figs. 4–6. Fig. 4 presents the dependence for compounds **1a–d** with increasing amounts of $LiCF_3SO_3$. All compounds increase their Φ_h–isotropic transition temperature ($T_{\Phi h-i}$) on their first DSC heating scan. A small decrease in the crystalline–Φ_h transition temperature ($T_{k-\Phi h}$) with the increase in the amount of complexed $LiCF_3SO_3$ is also observed. In the first cooling and second heating scans two differences can be seen as compared with the first heating scan. The first difference is that the $T_{k-\Phi h}$ of **1a** with only one oxyethylene segment is more kinetically controlled and occurs at lower temperatures than the corresponding transition of **1b**, **c** and **d**. Also, the $T_{k-\Phi h}$ transition temperature reaches a minimum at 0.18 mol of added $LiCF_3SO_3$. This behaviour is less noticeable for **1b**, **c** and **d**. The second difference is that the $T_{\Phi h-i}$ of **1c** and **d** shows different behaviour during the first cooling and second heating scans than in the first heating scan when greater than 0.8 mol of $LiCF_3SO_3$ are added. Previously we have found evidence of decomposition of **1** and **2** at elevated temperatures in the presence of $LiCF_3SO_3$.[4] Lewis-acid-catalysed cleavage of the phenyl benzyl ether groups by the $LiCF_3SO_3$ was suggested to be the cause of this degradation.[7]

As the number of oxyethylene segments in the molecule of **1** and **2** increases, the $T_{\Phi h-i}$ transition temperature decreases. With sequential addition of $LiCF_3SO_3$, **1c** and **d** have their $T_{\Phi h-i}$ systematically increased in the first heating scan at an approximately constant slope up to a concentration of 1.2 mol of $LiCF_3SO_3$ per mole of **1c** or **d**. Above this concentration which leads to $T_{\Phi h-i}$ values of 120 °C, decomposition of the complexes begins to occur. **1a** and **b** have smaller slopes than **1c** and **d** and are not able to complex as much $LiCF_3SO_3$ as **1c** and **d**. **1a** complexes only 0.3 mol of $LiCF_3SO_3$ in the Φ_h mesophase and **1b** complexes 0.4 mol of $LiCF_3SO_3$. Above these concentrations the $T_{\Phi h-i}$ is overlapped by a crystalline melting transition on the first heating scan which does not reform on the cooling scan but which is present also on the second heating scan. We do not fully understand this behaviour. DSC analysis indicates that a crystalline phase which has a higher $T_{k-\Phi h}$ than the pure **1a** or **b** may be induced by the high concentrations of $LiCF_3SO_3$. Optical polarized microscopy does not show any evidence of undissolved $LiCF_3SO_3$. Possibly this phase results from the formation of aggregates of $LiCF_3SO_3$ molecules within the assembled structure. Careful analysis by X-ray scattering experiments would be necessary to determine the nature of this phase or to elucidate whether a mixture of Φ_h and crystalline phases are present.

In contrast with **1a** and **b**, **1c** and **d** complex $LiCF_3SO_3$ in the Φ_h mesophase up to a concentration of 1.2 mol of salt per mole of **1**. Above this concentration which corresponds to $T_{\Phi h-i}$ of > 120 °C the molecules begin to decompose quite rapidly during the DSC experiments. As a result of this behaviour we could not determine the maximum amount of salt that could be complexed by **1c** and **1d**.

Fig. 5(*a*)–(*c*) show the phase behaviour of the polymers **2** *versus* the amount of complexed $LiCF_3SO_3$. **2a** and **2b** exhibit a $T_{\Phi h-i}$ on the first heating scan which is not detectable by DSC on the first cooling or second heating scans. The temperature of this transition decreases with the increasing amount of $LiCF_3SO_3$. The decrease in $T_{\Phi h-i}$ with the increasing amount of $LiCF_3SO_3$ is the opposite of the behaviour exhibited by **1a–d**. Both the decrease in $T_{\Phi h-i}$ with the increase in the amount of $LiCF_3SO_3$ and the absence of transition peaks on subsequent DSC scans probably result from the Lewis-acid-catalysed decomposition of the side-chain groups. **2c** and **d** exhibit the expected systematic increase in $T_{\Phi h-i}$ with sequential addition of $LiCF_3SO_3$ up to 0.4 mol of salt, and exhibit a Φ_h mesophase up to concentrations of 0.5 and 0.6 mol, respectively, per mole repeat of **2**. Above these concentrations **2c** and **d** do not display first-order phase transitions for the Φ_h–isotropic phase transition on their DSC scans. Fig. 5(*a*)–(*c*) demonstrate that both **2c** and **d** experience a decrease in their $T_{\Phi h-i}$ above concentrations of 0.4 mol of $LiCF_3SO_3$. This may result from some decomposition of the tapered polymer side groups, although the first-order transitions are detectable on subsequent DSC scans.

A comparison of the difference in the effectiveness of providing increased stabilization of the supramolecular organization for the Li cation with a radius of 0.68 Å[8] as compared to the Na cation with a radius of 0.97 Å[8] was made with **1c** and **d**. The experimental results are presented in Table 1 and plotted in Fig. 6(*a*)–(*c*). $T_{k-\Phi h}$ for both compounds gradually decreases with increasing salt concentration for both cations. However, $T_{\Phi h-i}$ systematically increases at the same rate for both cations providing almost identical Φ_h–isotropic phase transition temperatures for both sets of complexes. Irregular differences do become evident at high temperatures and salt concentrations where sample decomposition takes place (> 0.8 mol of added salt).

To help understand more clearly how the added salts provide increased stabilization to the Φ_h mesophase, molecular modelling was performed on **1a**, **d** and **2c** as well as on their complexes with $LiCF_3SO_3$. The results are shown in Fig. 7. Fig. 7(*a*) shows the cross-section of the self-assembled cylinder of **1a**. This arrangement has the polar oligooxyethylene segments in the centre of the arrangement and the non-polar alkyl tails at the column periphery. The alkyl tails are arbitrarily melted to achieve an average diameter of 44.8 Å which is consistent with X-ray scattering experiments of the Φ_h mesophase of **1a**.[4] The oxygen atoms of single oxyethylene segment of **1a** are indicated as the speckled atoms. Placed in the centre of the oligooxyethylene segments is a Li cation which is represented by the solid filled atom. With the high concentration of donor oxygen atoms (present as –OH groups) available in the centre of the assembly, this is the most probable site for complexation of the Li cation in the Φ_h mesophase.[9,10]

In comparison with **1a**, a model for the assembly of **1d** is shown in Fig. 7(*b*). **1d** Has four oxyethylene segments with four donor oxygen atoms per molecule available for coordination with the Li cations. The alkyl tails have been melted to an average diameter of 53.2 Å which is the diameter of the column formed by the uncomplexed **1d**. The oxyethylene segments are melted to fill the space of the core area efficiently. The arrangement shown in Fig. 7(*b*) is a two-dimensional (2-D) representation of **1d** in the Φ_h mesophase that is consistent with the experimental data obtained so far. This 2-D arrangement results in many high-energy conformations and unfavourable steric interactions. It is expected that the oxyethylene segments as well as the alkyl tails are rotated out of the plane of the cross-section along the column axis to avoid these conformations.

In the core of the column of **1d** there is a very high concentration of electron-rich donor oxygen atoms of the oxyethylene segments. Li cations are positioned within the Van der Waals radii of a minimum of two available oxygen atoms.[11] There are six Li cations present in the model which represents the highest concentration of $LiCF_3SO_3$ that was measured. It is expected that the oligooxyethylene segment will change its conformation so that the space is filled effectively and provides

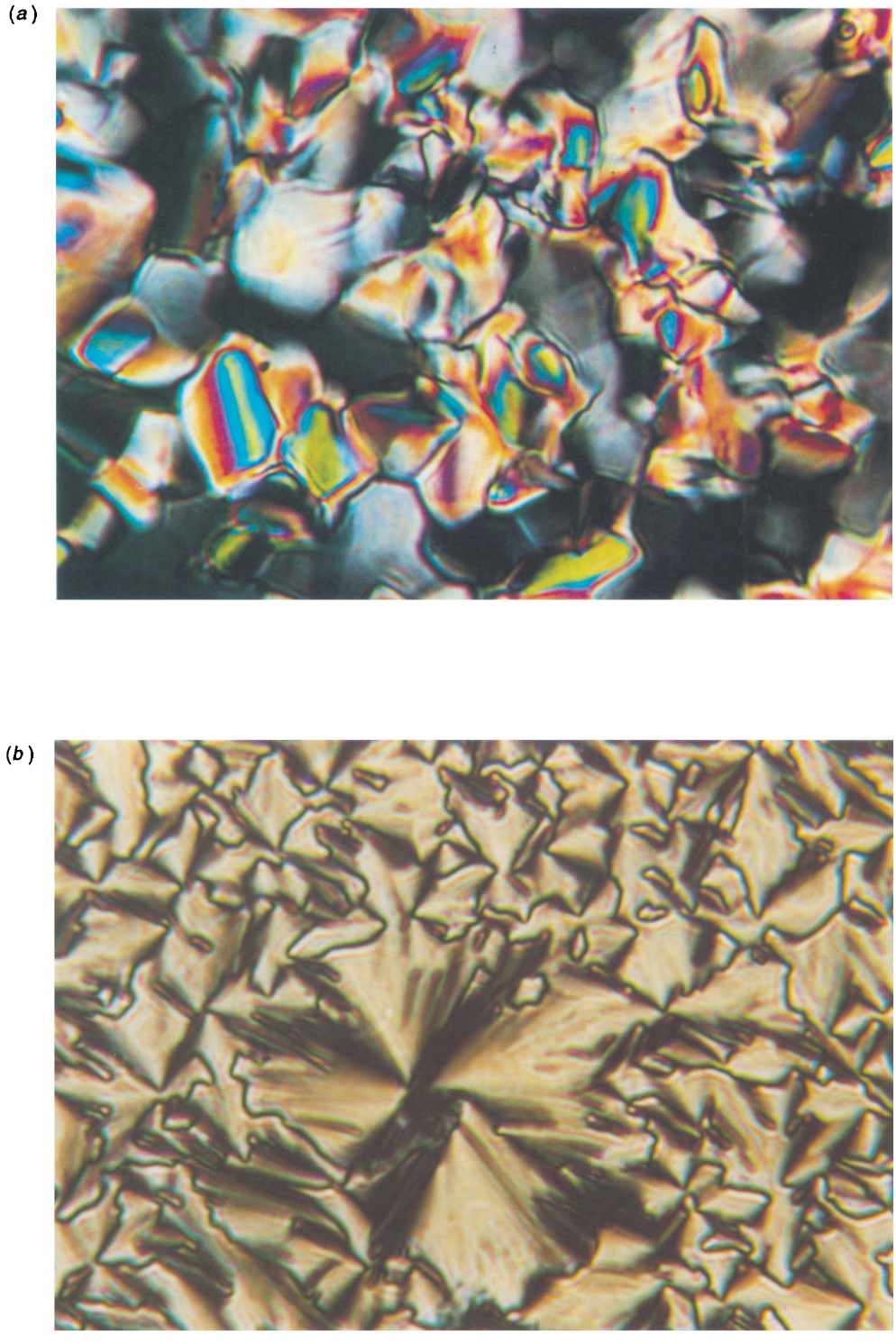

Fig. 3 Representative optical polarized micrographs of the texture exhibited by the hexagonal columnar (Φ_h) mesophase of: (*a*) **1a** upon cooling from 85 °C to 81 °C (1 °C min^{-1}); (*b*) **1d** upon cooling from 60 °C to 56 °C (1 °C min^{-1}); (*c*) **2c** upon cooling from 110 °C to 102 °C (1 °C min^{-1}) and annealing for 12 h; (*d*) **2c** with 0.4 mol of added $LiCF_3SO_3$ upon cooling from 125 °C to 110 °C (1 °C min^{-1}) and annealing for 12 h

(*c*)

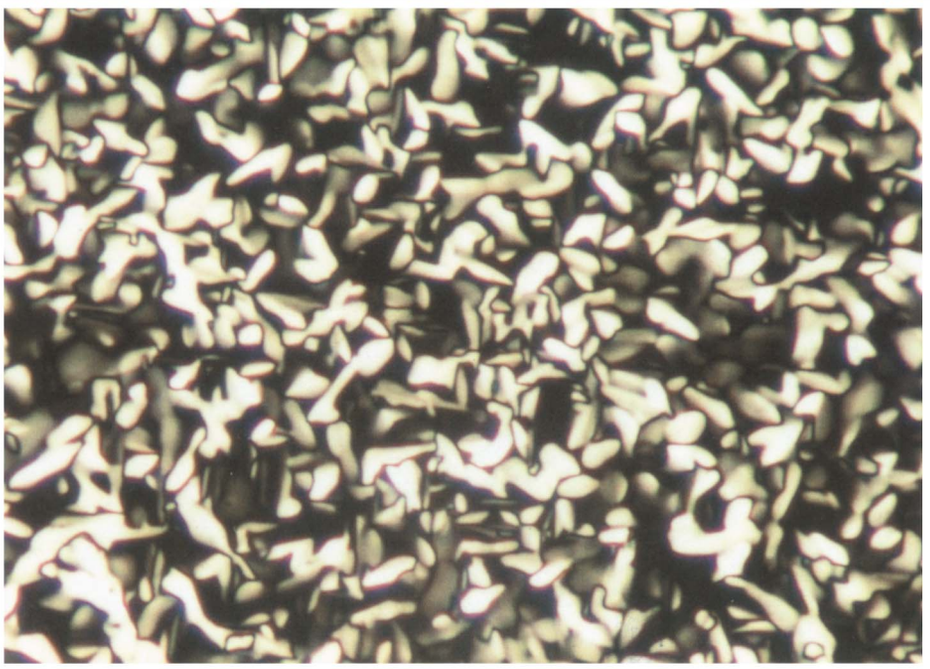

(*d*)

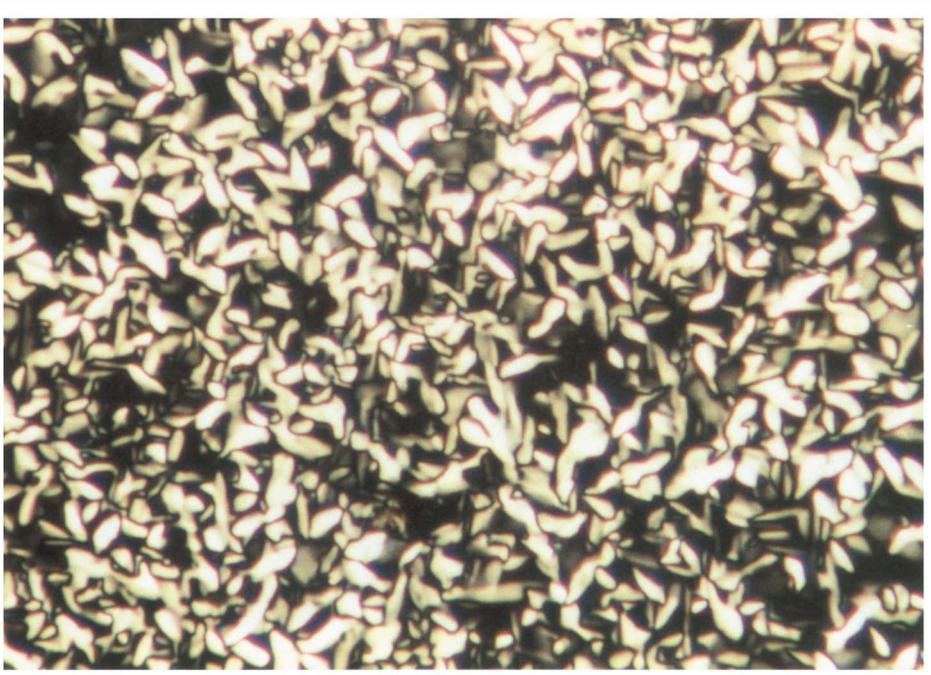

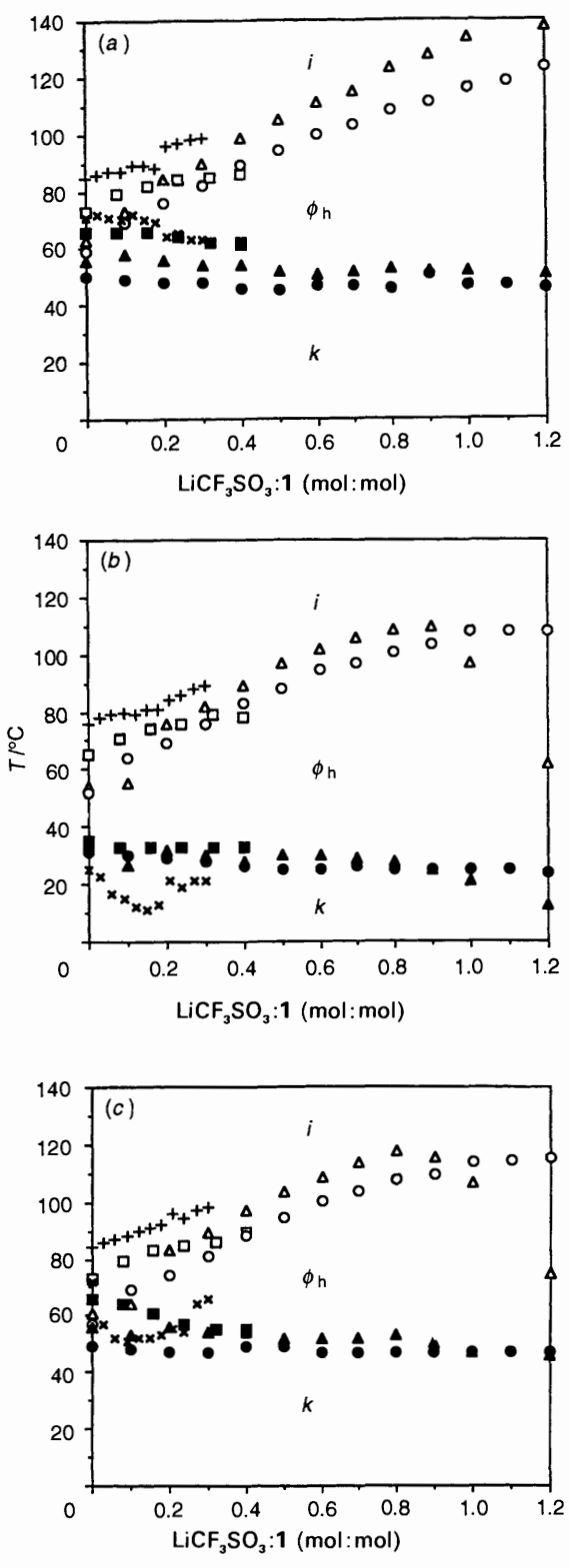

Fig. 4 The dependence of the k–Φ_h (T_m, filled symbols) and Φ_h–i (T_i, open symbols) phase-transition temperatures of the complexes of **1a** (+, ×), **1b** (□, ■), **1c** (△, ▲) and **1d** (○, ●) with various amounts of $LiCF_3SO_3$ (Table 1) obtained from: (*a*) the first DSC heating scans; (*b*) the first DSC cooling scans; (*c*) the second DSC heating scans

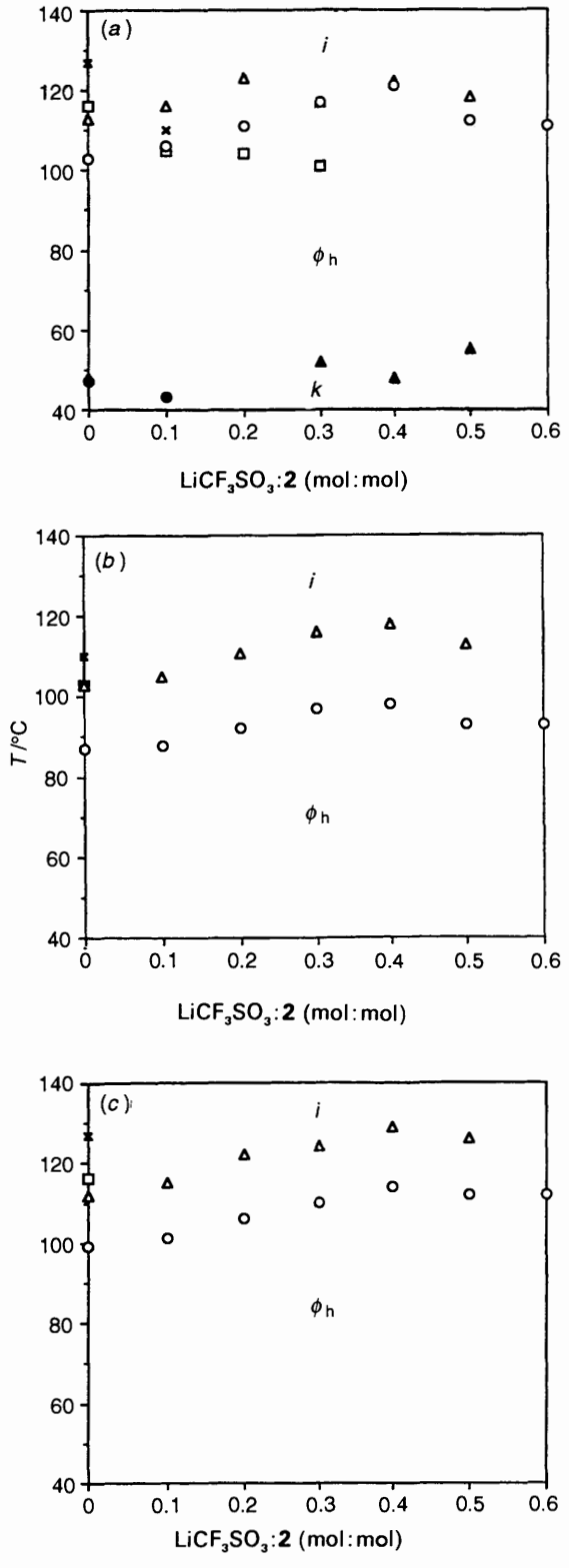

Fig. 5 The dependence of the k–Φ_h (T_m, filled symbols) and Φ_h–i (T_i, open symbols) phase-transition temperatures of the complexes of **2a** (×, +), **2b** (□, ■), **2c** (△, ▲), and **2d** (○, ●) with various amounts of $LiCF_3SO_3$ (Table 1) obtained from: (*a*) the first DSC heating scans; (*b*) the first DSC cooling scans; (*c*) the second DSC heating scans

the necessary coordination of the $LiCF_3O_3$ present. This interaction with the added salts provides the increased stabilization of the Φ_h mesophase up to higher temperatures (Table 1, Fig. 4).

The stabilization of the mesophase *via* complexation is probably the result of several factors. Speculation on two of the factors is possible based on these results. The increased ionic interactions that occur through the cooperative complexation of the added salts by the molecules of **1** in this cylindrically shaped assembly would provide enhanced rigidity of the oligooxyethylene column core. This would result in a decrease in the conformational entropy of the oligooxyethylene segments

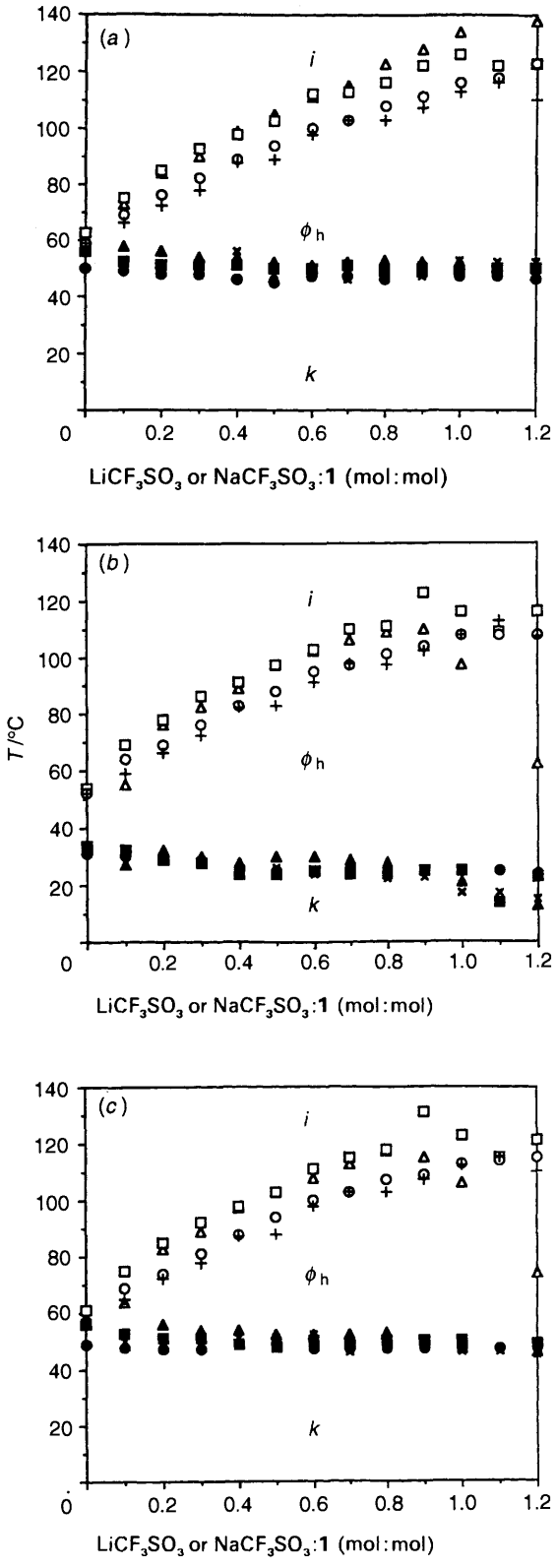

Fig. 6 The dependence of the k–Φ_h (T_m, closed symbols) and Φ_h–i (T_i, open symbols) phase-transition temperatures of the complexes of **1c** with various amounts of $LiCF_3SO_3$ (△, ▲) and $NaCF_3SO_3$ (□, ■) and of **1d** with various amounts of $LiCF_3SO_3$ (○, ●) and $NaCF_3SO_3$ (+, ×) (Table 1) obtained from: (*a*) the first DSC heating scans; (*b*) the first DSC cooling scans; (*c*) the second DSC heating scans

in the inner core of the column upon coordination with Li cations. This complexation provides a thermodynamic driving force to maintain this assembly at higher temperatures. The second factor is that the solvated salts convert the core of the cylinder from a polar region (resulting from the dipoles of oxyethylene segments)[12] into an ionic region with the dissolved salts. This provides an increase in the polarity of the cylinder core and may cause an enhancement of the hydrophobic interactions present in the assembly which stabilize it *via* microsegregation. Additional experiments which support these assumptions are in progress.

Fig. 7(*c*) shows a model of **2c** with the alkyl tails melted so that the column diameter matches the diameter determined by X-ray scattering experiments. This arrangement is based on the assumption that only a single polymer chain is present in the centre of the cylinder and that the cylinder formation must occur with cooperative conformational changes in the backbone conformation to allow the required positioning of the side groups to form the cylindrically shaped assembly. There is not yet any evidence to support or disprove this assumption. Li cations are positioned within the Van der Waals radii of a minimum of two available donor oxygens of the oxyethylene segments. As compared with the model of **1d** [Fig. 7(*b*)], the oxyethylene segments of **2c** are attached at one end to the polymer backbone and at the other end to the bulky taper shaped groups. The conformations available to oxyethylene segments are reduced as a result of the steric interactions of the tapered groups and the linear nature of the polymer backbone. Within a cross-section of the assembly, cooperative complexation of Li cations by the oxyethylene segments of adjacent side groups appears less likely to occur as a result of steric interactions. Complexation of the cation possibly occurs to a greater extent between the oxyethylene segments of repeat units which are stacked on top of each other along the column axis.

The positional restrictions imposed by the covalent attachment to the polymer backbone limit the amount of added $LiCF_3SO_3$ that can be complexed as well as the magnitude of the increase in $T_{\Phi h-i}$ per increase of added $LiCF_3SO_3$. For example, **1c** with 0.4 mol of added $LiCF_3SO_3$ has a $T_{\Phi h-i}$ which is 36 °C higher than the pure uncomplexed **1c**. Comparatively, **2d** has only an 18 °C increase in $T_{\Phi h-i}$ with the addition of the same amount of $LiCF_3SO_3$ (**1c** and **2d** are compared since they both have three donor oxygen atoms in the oxyethylene spacer available for complexation). The oxyethylene segments and the tapered side groups, most likely as a result of steric interactions, appear not to have the mobility to adjust positions and conformations in order to take advantage of the increased ionic interactions in providing stabilization to the cylindrically shaped assembly. This observation is further illustrated by noting that compound **1c** eventually has $T_{\Phi h-i}$ increased 11 °C higher than any of the polymers **2** at any of the concentrations measured (determined from the first DSC heating scans).

Conclusions

The low molecular weight compounds **1** are able to complex higher concentrations of $LiCF_3SO_3$ in their self-assembled cylindrically shaped architecture which displays a Φ_h mesophase with greater increases in $T_{\Phi h-i}$ per increase in salt concentration than the corresponding polymethacrylates **2** derived from them. Based upon molecular modelling, positional and conformational restrictions imposed by both the tapered side groups and the polymer backbone are suggested for the explanation of these results. For both **1** and **2**, increasing the number of oxyethylene segments present in the flexible spacer shifts $T_{\Phi h-i}$ to lower temperatures and allows more $LiCF_3SO_3$ to be complexed in their cylindrically shaped assembly. A comparison of the difference in the effectiveness of the Li cation *versus* the Na cation in providing increased stabilization of the Φ_h mesophase does not show, to within the experimental error, significant differences between the two cations.

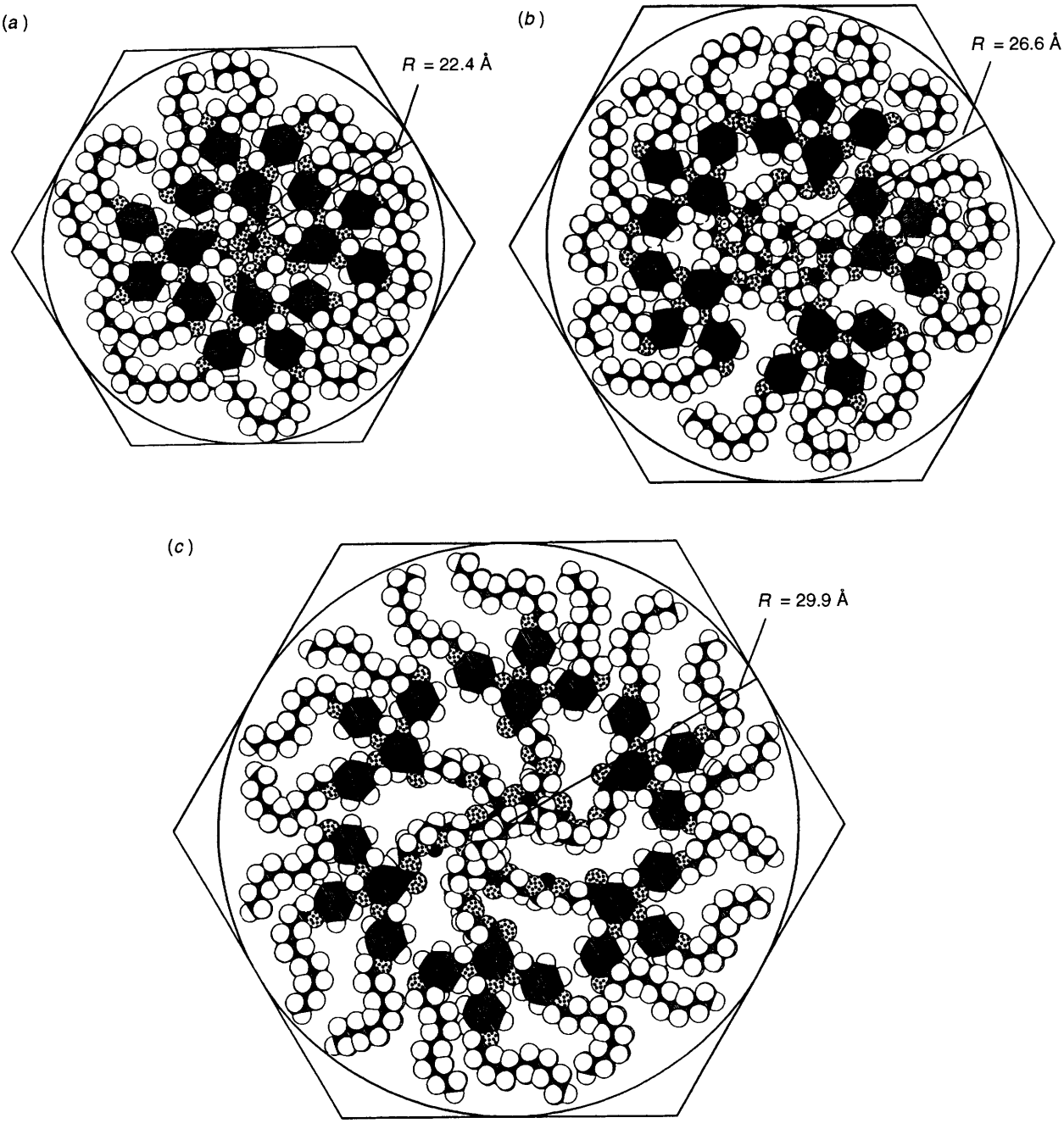

Fig. 7 Schematic representation of a cross-section of the supramolecular cylinders of **1** and **2** in the Φ_h mesophase with Li cations (●) complexed by the oxygen atoms of the oxyethylene segments and the alkyl tails melted to match the column radius determined by X-ray scattering experiments: (*a*) top view of the cylinder containing four molecules of **1a** in a stratum; (*b*) top view of the cylinder containing five molecules of **1d** in a stratum; (*c*) top view of a cylinder of **2c** containing six repeat units in a stratum

Acknowledgements

Financial support from the National Science Foundation (DMR-92-06781) and the Office of Naval Research, and a NATO travelling grant are gratefully acknowledged.

References

1 (*a*) J. M. Lehn, *Angew. Chem., Int. Ed. Engl.*, 1988, **27**, 89; (*b*) J. M. Lehn, *Angew. Chem., Int. Ed. Engl.*, 1990, **29**, 1304; (*c*) J. S. Lindsey, *New J. Chem.*, 1991, **15**, 153; (*d*) G. M. Whitesides, J. P. Matias and C. T. Seto, *Science*, 1991, **254**, 1312; (*e*) eds. H. J. Schneider and H. Durr, *Frontiers in Supramolecular Chemistry*, Wiley, New York, 1992; (*f*) eds. V. Balzani and L. DeCola, *Supramolecular Chemistry*, Kluwer, Dordrecht, 1992; for a series of books on supramolecular chemistry see: (*g*) series ed. J. F. Stoddart, *Monographs in Supramolecular Chemistry*, Royal Society of Chemistry, Cambridge, 1991; (*h*) series ed. G. W. Gokel, *Advances in Supramolecular Chemistry*, vol. 1, 1991 and vol. 2, 1992, JAL Press, London; (*i*) ed. S. M. Roberts, *Molecular Recognition: Chemical and Biochemical Problems*, Part I, 1989 and Part II, 1992, Royal Society of Chemistry, Cambridge; (*j*) F. Vögtle, *Supramolecular Chemistry*, Wiley, New York, 1991.

2 (*a*) J. Rebek Jr., *Angew. Chem., Int. Ed. Engl.*, 1990, **29**, 245; (*b*) D. Philip and J. F. Stoddart, *Synlett*, 1991, 445.

3 V. Percec, G. Johansson, J. Heck, G. Ungar and S. V. Batty, *J. Chem. Soc., Perkin Trans. 1*, 1993, 1411.

4 V. Percec, J. Heck, D. Tomazos, F. Falkenberg, H. Blackwell and G. Ungar, *J. Chem. Soc., Perkin Trans. 1*, in the press.

5 (*a*) V. Percec, M. Lee, J. Heck, H. Blackwell, G. Ungar and A. Alvarez-Castillo, *J. Mater. Chem.*, 1992, **2**, 931; (*b*) V. Percec, J. Heck, M. Lee, G. Ungar and A. Alvarez-Castillo, *J. Mater. Chem.*, 1992, **2**, 1033.

6 V. Percec, G. Johansson and R. Rodenhouse, *Macromolecules*,

1992, **25**, 2563; (*b*) V. Percec and G. Johansson, *J. Mater. Chem.*, 1993, **3**, 83; (*c*) V. Percec and D. Tomazos, *J. Mater. Chem.*, 1993, **3**, 633; (*d*) V. Percec and D. Tomazos, *J. Mater. Chem.*, 1993, **3**, 643.

7 (*a*) J. Collomb, P. Arland, A. Gandini and H. Cheradame, in *Cationic Polymerization and Related Processes*, ed. E. J. Goethals, Academic Press, New York, 1984, p. 49 and references cited therein; (*b*) Y. Eckstein and P. Dreyfuss, *J. Inorg. Chem.*, 1981, **43**, 23; (*c*) A. Loupy and B. Tchouber, *Salt Effects in Organic and Organometallic Chemistry*, VCH, Weinheim, 1992, p. 2; (*d*) R. M. Pagni, G. W. Kabalka, S. Bains, M. Plesco, J. Wilson and J. Bartmess, *J. Org. Chem.*, 1993, **58**, 3130.

8 R. C. Weast, ed., *CRC Handbook of Chemistry and Physics*, 65th edn., CRC Press, Inc., 1984.

9 The results of NMR experiments of polyethylene oxide dimethyl ethers suggest that the Li cation is coordinated by not more than four oxygen atoms for solvent-separated ion pairs, see: (*a*) L. L. Chan and J. Smid, *J. Am. Chem. Soc.*, 1967, **89**, 4547; (*b*) J. Smid, *Angew. Chem., Int. Ed. Engl.*, 1972, **11**, 112.

10 NMR measurements and binding constants for polyethylene oxide derivatives support the conclusion that the terminal hydroxy group of polyethylene glycols plays an important role in the complexation of metal cations, see: (*a*) S. Yanagida, K. Takahashi and M. Okara, *Bull. Chem. Soc. Jpn.*, 1978, **51**, 1294, 3111; (*b*) G. W. Gokel, D. M. Goli and R. A. Schultz, *J. Org. Chem.*, 1983, **48**, 2837; (*c*) eds. F. Vögtle and E. Weber, *Host–Guest Complex Macrocycles: Synthesis, Structures, Applications*, Springer-Verlag, Berlin, 1985.

11 In the crystal structure of the complex of tetraethylene glycol dimethyl ether with $CdCl_2$, it was shown that an oxygen atom may function as a bridge between two metal cations and therefore provide complexation for more than one cation at a time, see: R. Iwamoto and H. Wakano, *J. Am. Chem. Soc.*, 1976, **98**, 3764.

12 (*a*) T. Uchida, Y. Kurita, N. Koizumi and M. Kubo, *J. Polym. Sci.*, 1956, **21**, 313; (*b*) W. J. Svirbely and J. L. Lander, *J. Am. Chem. Soc.*, 1945, **67**, 2189; (*b*) C. P. Smyth and W. S. Walls, *J. Am. Chem. Soc.*, 1931, **53**, 2115.

Paper 3/03884J
Received 6*th July* 1993
Accepted 26*th July* 1993